

Automatic microfluidic platform for cell separation and nucleus collection

Chien-Hsuan Tai · Suz-Kai Hsiung · Chih-Yuan Chen ·
Mei-Lin Tsai · Gwo-Bin Lee

Published online: 17 May 2007
© Springer Science + Business Media, LLC 2007

Abstract This study reports a new biochip capable of cell separation and nucleus collection utilizing dielectrophoresis (DEP) forces in a microfluidic system comprising of micropumps and microvalves, operating in an automatic format. DEP forces operated at a low voltage ($15 V_{p-p}$) and at a specific frequency (16 MHz) can be used to separate cells in a continuous flow, which can be subsequently collected. In order to transport the cell samples continuously, a serpentine-shape (S-shape) pneumatic micropump device was constructed onto the chip device to drive the samples flow through the microchannel, which was activated by the pressurized air injection. The mixed cell samples were first injected into an inlet reservoir and driven through the DEP electrodes to separate specific samples. Finally, separated cell samples were collected individually in two outlet reservoirs controlled by microvalves. With the same operation principle, the nucleus of the specific cells can be collected after the cell lysis procedure. The pumping rate of the micropump was measured to be $39.8 \mu\text{l}/\text{min}$ at a pressure of 25 psi and a driving frequency of 28 Hz. For the cell separation process, the initial flow rate was $3 \mu\text{l}/\text{min}$ provided by the micropump. A throughput of 240 cells/min can be obtained by using the developed device. The DEP electrode array, microchannels, micropumps and microvalves are integrated on a microfluidic chip using micro-electro-mechanical-systems (MEMS) technology to perform several crucial procedures including cell transportation,

separation and collection. The dimensions of the integrated chip device were measured to be 6×7 cm. By integrating an S-shape pump and pneumatic microvalves, different cells are automatically transported in the microchannel, separated by the DEP forces, and finally sorted to specific chambers. Experimental data show that viable and non-viable cells (human lung cancer cell, A549-luc-C8) can be successfully separated and collected using the developed microfluidic platform. The separation accuracy, depending on the DEP operating mode used, of the viable and non-viable cells are measured to be 84 and 81%, respectively. In addition, after cell lysis, the nucleus can be also collected using a similar scheme. The developed automatic microfluidic platform is useful for extracting nuclear proteins from living cells. The extracted nuclear proteins are ready for nuclear binding assays or the study of nuclear proteins.

Keywords Dielectrophoresis force · Micropump · Microvalve · Cell separation · Cell collection · MEMS · Microfluidics

Nomenclature

AC	Alternating current
Bio-MEMS	Bio-micro-electro-mechanical-systems
DEP	Dielectrophoresis
DMEM	Dulvecco's modified eagle medium
DNA	Deoxyribonucleic acid
EMV	Electromagnetic valve
ER	Estrogen nuclear receptor
LIF	Laser induced fluorescence
LOC	Lab-on-a-chip
MEMS	Micro-electro-mechanical-systems
PDMS	Polydimethylsiloxane
PI	Propidium iodide

C.-H. Tai · S.-K. Hsiung · G.-B. Lee (✉)
Department of Engineering Science,
National Cheng Kung University, Tainan, Taiwan 701
e-mail: gwobin@mail.ncku.edu.tw

C.-Y. Chen · M.-L. Tsai
Department of Physiology, National Cheng Kung University,
Tainan, Taiwan 701

PR	Photoresist
SEM	Scanning electron microscope
S-shape	Serpentine-shape
V_{p-p}	Peak-to-peak Voltage

1 Introduction

Application of long-term anti-estrogen therapy (such as tamoxifen) by targeting estrogen nuclear receptor (ER) in tumors can effectively control early-stage breast cancer growth (Ring and Dowsett 2004). Two important steps to discover the lead compounds as anti-estrogen agents include cell viability assays and the binding assays of activated nuclear receptors to a specific DNA motif. However, the long process in discovering anti-estrogen related compounds has hindered its practical applications for candidate drugs. To shorten the process of identifying the lead compounds, automatic analysis for cell viability and nuclear receptor binding assays should be of great need.

Up to date, automatic analysis for cell cytotoxicity has been reported (Skehan et al. 1990). However, the nuclear protein binding assay has not yet reported. Ideally, automatic analysis of the nuclear binding assay requires a platform which can collect sufficient amounts of cell nucleus from living cells and separate the complex of estrogen nuclear receptors and DNA motif from unbound DNA motif. Since modified glass-based capillary electrophoresis microchips have been developed to separate the complex of estrogen nuclear receptors from unbound DNA motif effectively (Chuang et al. 2006), the crucial step left for automatic analysis of nuclear receptor binding is to develop a device which can collect nuclear proteins from the living cells.

There is a great need for miniature devices and systems to provide precise and high-throughput analysis and characterization of biological samples such as cells and micro-organisms (Auerswald and Knapp 2003; Doh and Cho 2005). Bio-MEMS (bio-micro-electro-mechanical-systems) technologies based on the principles of biology, analytical chemistry and miniaturization techniques have proven to be a promising approach to realize the so-called lab-on-a-chip (LOC). By integrating several critical miniature components on a single chip, a biochip system can perform functions such as transporting, preparation, handling, reaction, mixing, separation, and detection for sample analysis and characterization. Typically, LOC systems possess advantages including lower sample/reagent consumption, higher throughput, higher sensitivity and resolution, and lower unit cost and power consumption (Ziaie et al. 2004; Sato et al. 2003; Chiem and Harrison 1998; Raiteri et al. 2002; Jaln 2000). In order to accomplish

the abovementioned functions, a typical biochip system is designed to be composed of several microfluidic devices, including micropumps, microvalves, and microchannels for bio-sample transportation and control. Previous studies have investigated the ability of bio-chip systems to perform a wide scope of biological applications including cell culture monitoring, cell lysis, protein/DNA separation, DNA/reagent mixing and DNA amplification (Reyes et al. 2002; Auroux et al. 2002).

The concepts of microfluidic devices for handling a minute amount of fluids have been widely investigated since micropumps structures were first demonstrated in the early 1980s (Laser and Santiago 2004). With different actuation principles, different challenges exist in the fabrication and applications of micropumps (Zengerle et al. 1995; Manz et al. 1991). In order to simplify the fabrication of the micropumps device, the concept of pneumatic micropumps driven by compressed air supplied by an external source has attracted considerable interest (Unger et al. 2000). Typically, three membranes are activated peristaltically to generate pumping effect. Pneumatic microfluidic devices provide an effective and reliable method to handle fluids in microchannels and can be easily integrated onto the bio-analysis chips (Wang and Lee 2005).

Collection of living/viable cells is essential for separating and concentrating specific proteins from subcellular organelles such as nuclear proteins (Becker et al. 1995; Li and Bashir 2002; Zou et al. 2006; Markx et al. 1994; Huang et al. 1992). When compared with traditional biological methods such as flow cytometry (Brown and Wittwere 2000; Tazzari et al. 2003; Widrow et al. 1997; Widrow and Laird 2000), dielectrophoresis (DEP) provides a promising approach to separate cells with different dielectric properties (Gascoyne et al. 1997). DEP is a method that can exploit changes in cell dielectric properties to create a force that can be used to physically move cells (Pohl 1978; Fu et al. 2004). Biological samples and inorganic microparticles can be attracted into a region with a maximum electrical field intensity by a positive DEP effect or repelled into a region with a minimum electrical field intensity by a negative DEP effect (Becker et al. 1995; Gascoyne et al. 1997). The basis for cell separation by DEP is the movement of ions in an applied alternating electrical field around and within the cell samples up to biological membranes (Wang et al. 1994). DEP forces have been demonstrated to be capable of separating various cells (Auerswald and Knapp 2003). The feasibility of using DEP for separating and trapping sub-micrometer-scale bio-particles has also been reported (Schnelle et al. 2000). Notably, most of the previous studies used DEP forces to separate cells in a stagnant flow. In order to increase the cell separation throughput, large-scale pumping devices such as syringe pumps are usually used to transport samples for cell separation in a continuous flow.

In this study, we demonstrate an automatic microfluidic platform for living cell separation and nucleus collection utilizing DEP forces in a continuous flow. The microfluidic system is composed of microchannels, a pneumatic micropump, four microvalves, and a DEP microelectrode array. By using MEMS fabrication technology, microfluidic devices can be integrated onto the biochip to achieve the functions of cell transportation, separation and collection. DEP forces operated at a low voltage and at a specific frequency applied on the microelectrode array can be used to separate cells and nuclei in a continuous flow. The micropump and microvalves are used to control the flow motion such that certain parts of cells can be transported to subsequent cell collection chambers. In order to demonstrate the capability of the developed system, human lung cancer cells were used for testing. Furthermore, the nuclei can be also separated after cell lysis process, and then collected using a similar approach with the developed microfluidic device.

2 Materials and methods

2.1 Design

In order to perform the cell/nucleus separation and collection automatically, several micro-scale components were integrated onto the microfluidic chip device. Figure 1

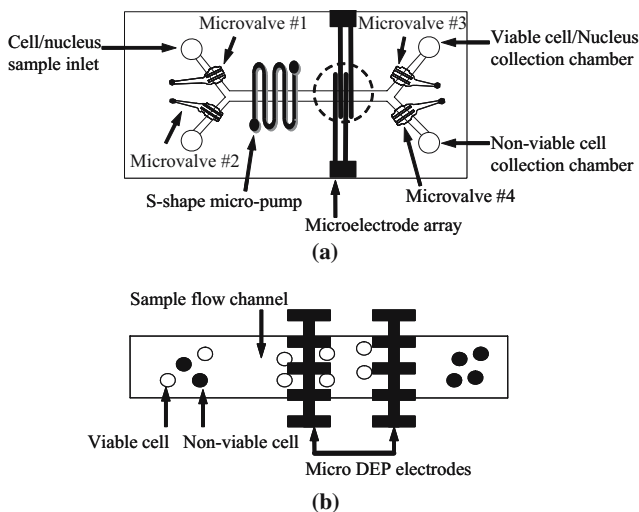


Fig. 1 (a) Schematic illustration of the automatic cell/nucleus separation and collection chip. Several components including a microchannel, an S-shape micropump, four microvalves and DEP microelectrode array are integrated onto a single chip. (b) Schematic illustration of the working principle of the DEP microelectrode array. When positive DEP forces are generated, viable cells are captured on the surface of the microelectrode array. Then non-viable cells are moved into the non-viable cell collection chamber continuously by using the micropump and microvalves

presents a schematic illustration of the operating principles of the automatic microfluidic system for cell/nucleus separation and collection. As can be clearly seen in Fig. 1(a), several crucial microfluidic components such as microchannels, a micropump, four microvalves and the DEP microelectrode array are integrated onto the chip device. A pneumatic serpentine-shape (S-shape) pump and four microvalves were used to control the flow motion such that mixed cell samples suspended in the medium can be transported into the micro-channel and moved to specific collection chambers automatically. In order to achieve cell separation and collection, the integrated DEP microelectrode array applies DEP forces on specific cells. Note that four microvalves were used to control the sample flow direction. After the DEP electrode array was activated, positive DEP forces were generated and viable cells were attracted to the electrodes. Non-viable cells were continuously removed and collected into the collection chamber. In this study, a design of S-shape micropump was used for fluid transportation (Wang and Lee 2006; Yang et al. 2006). As the compressed air travels along the upper S-shape microchannel, it causes the polydimethylsiloxane (PDMS) membranes to deflect. The time-phased deflection of successive membranes along the microchannel length generates a peristaltic effect that drives the fluid along the microfluidic channel. With this approach, the fluid flow can be driven using only a single electromagnetic valve (EMV, SMC Inc., S070M-5BG-32, Japan) switch regulated by a simple circuit. Figure 1(b) shows the working principle of the DEP microelectrode array. The mixed viable and non-viable cells were first transported to the electrode-array region. While the AC electric field was applied on the electrode structure, positive and negative DEP forces were induced onto the viable and non-viable cells, respectively, depending on the conductivity and permittivity of cells and the fluid medium. The positive DEP force was generated on the viable cells. They were captured on the surface of the microelectrode array. Then the non-viable cell samples can be continuously transported into the collection chamber with a high-throughput. After the collection of non-viable cells, the supply of the electric field was terminated, the microvalves were activated, and the viable cell samples were released and then transported into another collection chamber. Therefore, it completes the separation process of the cell samples. Moreover, after cell separation, the nucleus can be also separated from the membranes and cytoplasm and collected using a similar approach if positive DEP forces are applied for nucleus attraction. These nuclei can be collected for subsequent analysis and processing.

For the purpose of the purification of the cell samples after culture process, the cell samples including viable and non-viable cells were first injected into the reservoir. While

Table 1 Operation sequence of the pneumatic microvalves during different stages

Stage #	Microvalve #			
	#1	#2	#3	#4
Stage 1	•		•	
Stage 2	•	•		•
Stage 3	•			•
Stage 4		•	•	•

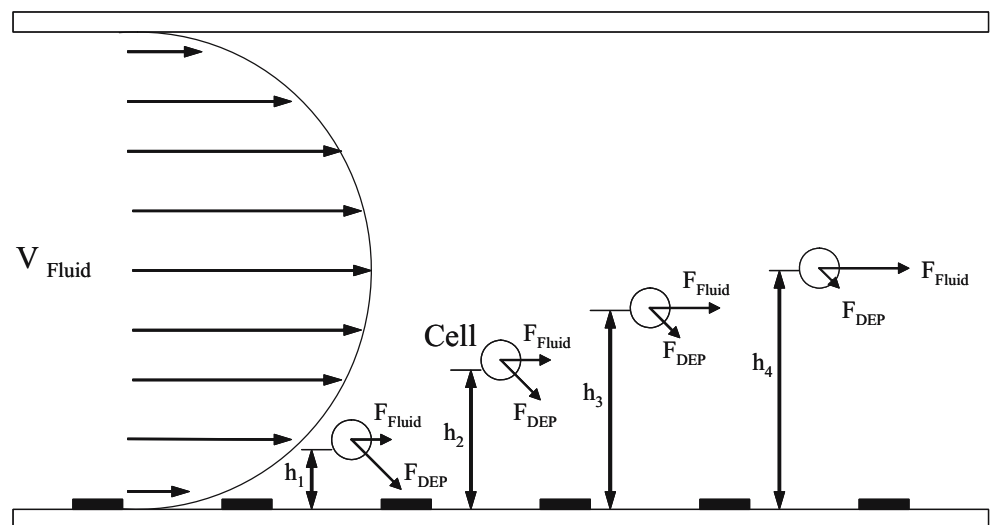
the AC power with specific voltage and frequency applied on the microelectrode, positive DEP force can be generated to capture the viable cells so that negative DEP force can be generated to repel the non-viable cells. To extract the protein from the nucleus, the purification process of the nuclei was required. After a standard boiling thermal cell lysis process, the nuclei can be released from the membranes. The transportation direction of the pneumatic micro-pump can be reversed by applying the compressed air from the other air inlet. Similarly, the nuclei can be captured on the surface of the microelectrode array by the positive DEP force while the AC power with different frequency was applied onto the microelectrode. Finally, the nuclei of the target cells can be separated and collected by using the developed chip.

By utilizing different operation sequence of the pneumatic microvalves (as shown in Table 1), the viable and non-viable cell samples can be separated into two different reservoirs. Four stages were utilized to achieve the separation and collection of both the viable cells and nuclei. First, the microvalve #1 and 3 can be actuated while compressed air was injected (stage 1). The flow direction can be controlled and guided the non-viable cell samples

into non-viable cell collection chamber. After the release of the viable cells from the microelectrode array region, microvalve #1, 2 and 4 were actuated to guide the viable cells flow into the viable cell collection chamber (stage 2). For the purpose of DNA/protein extraction, the thermal cell-lysis process was employed, and the nuclei and other organelles can be transported to the microelectrode array region using the micro-pump. The plasma membrane and other organelles can also be collected while microvalve #1 and 4 were actuated (stage 3). Finally, the collection of target nuclei can be completed after the actuation of microvalve # 2, 3, and 4.

2.2 Mathematical model

DEP forces can be used for the movement of particles/cells in a non-uniform electric field as a tool for cell/particle separation and manipulation. It was first used for manipulation of suspended particles in an organic medium (Pohl 1958). Particles/cells may be moved, trapped, collected, aligned, or even rotated using induced dipole moments generated by microelectrodes. When particles/cells are suspended in a spatially non-uniform electric field, the applied electric field induces a dipole moment in the particles/cells. The interaction of the electric field with the induced charges on either side of the dipole generates a net force. Due to the inhomogeneous nature of the electric field, if the particle/cell is more polarizable than the medium surrounding it, the dipole aligns with the electric field and there is a net motion towards the region with a higher electric field. This effect is called “positive DEP.” Conversely, if the particle/cell is less polarizable than the surrounding medium, the dipole aligns against the electric field and the particle is repelled from the higher electric field region, resulting in a so-called “negative DEP.”

Fig. 2 Schematic illustration of cells experiencing positive DEP forces

When decreasing the scale of the dielectrophoretic devices, dielectrophoretic forces can be increased because of increasing electrical field (Bahaj and Bailey 1979) as described below.

$$F_{DEP} \propto \frac{V^2}{L_e^3} \quad (1)$$

where F_{DEP} is the dielectric force, V is the applied voltage and L_e is the length between electrodes. Therefore, miniaturization of DEP devices can significantly enhance the magnitude of the dielectrophoretic forces exerted on a particle/cell.

A positive DEP force was used to attract the cells on the electrodes (Pohl 1978). The DEP force experienced by a cell in a non-uniform electric field can be represented by the following equation (Jones 1995):

$$F_{DEP} = 2\pi\epsilon_m r^3 \text{Re}[f_{cm}] \nabla E_{rms}^2 \quad (2)$$

where r is the radius of the cell; ϵ_m is the permittivity of the medium; f_{cm} is the Clausius–Mossotti factor; E_{rms} is the root mean square value of an electric field. $\text{Re}[f_{CM}]$ means the real part of the f_{CM} , which can be represented as follows (Pohl 1951; Huang et al. 2001):

$$f_{cm} = \frac{\epsilon_p^* - \epsilon_m^*}{\epsilon_p^* + 2\epsilon_m^*} \quad (3)$$

where ϵ^* is the complex permittivity ($\epsilon^* = \epsilon - j\sigma/\omega$); σ is the conductivity; ω is the electric field frequency. Subscripts p and m delineate the cell and the medium, respectively. If $\text{Re}[f_{CM}] > 0$, the cell experiences a positive DEP force. Conversely, while $\text{Re}[f_{CM}] < 0$, cell experiences a negative DEP force. In this study, cells moving in a microchannel experiences positive DEP forces and finally attached on the electrodes (as shown in Fig. 2). If the cell is initially located near the channel wall, it experiences a higher attractive force and will be moved towards the electrodes. For cells moving at a higher velocity, they are far away from the electrode and experience a smaller DEP force, these cells may not be attracted on the electrodes and cannot be separated successfully.

Appreciable heating can be observed for large-scaled DEP devices due to the high voltages required to accomplish dielectrophoresis (Jones 2003). Heating is remarkably reduced when DEP devices are miniaturized (Gonzalez and Remcho 2005).

2.3 Fabrication

Figure 3 presents a simplified fabrication process for the automatic microfluidic device for cell/nucleus separation and collection (AMD-CNSC). The manufacturing process

comprises two major steps, namely fabrication of the microelectrode structure and formation of the PDMS microfluidic structure. A detailed description of the fabrication process is provided in the following sections.

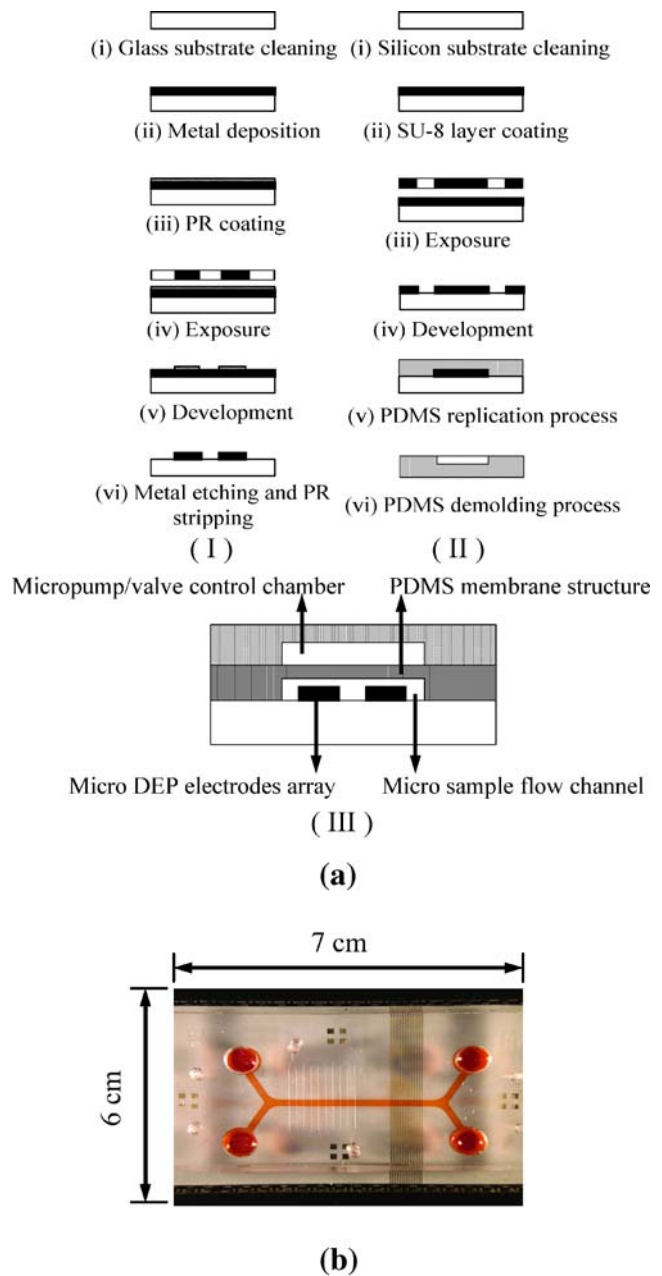


Fig. 3 The overview of the fabrication process for the automatic cell/nucleus separation and collection chip. **(a)** (I) The fabrication process of the microelectrode array structure. **(a)** (II) The simplified fabrication process of the SU-8 master mold and the replication process of the PDMS chip. **(a)** (III) Cross-section view of the microfluidic chip. **(b)** Photograph of the cell/nucleus separation and collection device. The width and length of the chip are 6 and 7 cm, respectively

2.4 Fabrication of the microelectrode structure

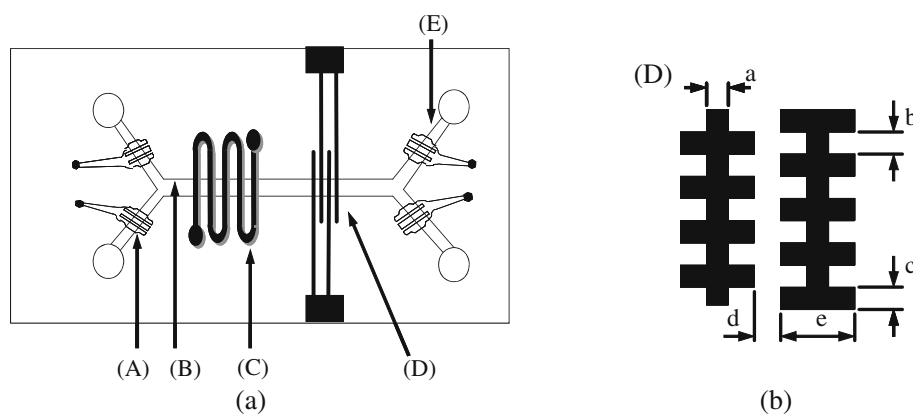
Figure 3(a)-I represents the fabrication process of the microelectrode array structure. The present study employed polished soda–lime glass substrates (G-Tech Optoelectronics Corp., Taiwan) and a standard lithography and metal etching process to fabricate the microelectrode array (Lee et al. 2005). Briefly, the microelectrode array structure for DEP force generation was fabricated on the surface of a 3-mm-thick soda-lime glass substrate. Initially, a thin chrome film with a thickness of 1,000 Å as an adhesive layer was deposited. Then a gold film with a thickness of 3,000 Å was deposited on top of the chrome film. To define the pattern of the underlying chrome and gold layers, a thin layer of AZ4620 (Clariant, USA) positive photoresist (PR) was then spun on the substrate to form an etching mask. Hence, the geometry of the microelectrode array could be well defined.

2.5 Formation of the PDMS microfluidic structure

For the formation of the PDMS microfluidic structure, a SU-8 photoresist (MicroChem Corp., MA, USA) master mold was formed onto silicon substrates. Figure 3(a)-II shows a simplified fabrication process of the SU-8 master mold and the replication process of the PDMS structure. A

detailed fabrication process can be found in our previous work (Wang and Lee 2006). SU-8 is a suitable material for the master mold of the PDMS casting process due to its excellent structural robustness, good adhesion onto the silicon substrate, and easy production of high-aspect-ratio structures (Lin et al. 2002). After the fabrication process of the SU-8 master mold, PDMS-based chip device with the inverse structures of the SU-8 master mold could be formed after a de-molding process (Anderson et al. 2000; Duffy et al. 1998). In order to construct the actuation membranes of the S-shape pneumatic micropump, a PDMS thin film spin-on process was then performed and a membrane structure can be generated onto the PDMS chip device (Wang and Lee 2006). Figure 3(a)-III represents a cross-section view of the developed chip device. It can be clearly seen that the chip device comprises of three major parts, including pump/valve control chambers and liquid microchannels, PDMS membrane structures, and a microelectrode array fabricated on the glass substrate. These three parts were bonded together to form a sealed microchannel structure by using oxygen plasma treatment. A photograph of the assembled microfluidic chip is shown in Fig. 3(b). The width and length of the chip are measured to be 6 and 7 cm, respectively. A detailed information of the dimensions of the developed device was shown in Table 2.

Table 2 Dimensions of the components integrated onto the microfluidic device



A	Microvalve	Depth:100 μm , Width:500 μm Width of widest area: 1 mm Distance between two fingers: 100 μm
B	Micro flow channel	Depth:100 μm , width:1 mm
C	S-shape micropump	Depth:100 μm , width:500 μm Distance between two neighboring intersection areas: 500 μm
D	Microelectrode	a : 30 μm , b : 50 μm , c : 30 μm , d : 50 μm , e : 90 μm
E	Microvalve channel	Depth: 100 μm , width: 1 mm

2.6 Sample preparation

The cell samples used in the experiment are human lung cancer cells (A549-luc-C8, ATCC, USA) with an average diameter of 15 μm . The cell samples were first incubated in the DMEM (Dulvecco's modified eagle medium) buffer (HyClone Corp., USA) containing 2 mM L-glutamine, 1.5 g/l sodium bicarbonate, 10% fetal bovine serum (FBS, no. 26140-079, Gibco, CA), 100 units/ml of penicillin and streptomycin (no. 15140-122, Gibco, CA) under 37°C and 5% CO_2 for 72 h. After the cell culture process, a solution including Trypsin and 0.5 mM EDTA (ethylenediaminetetraacetic acid) was used to detach the cells from the substrate. Then a centrifuge was used to separate the cell samples from the solution. The cell samples were then suspended into fresh DMEM buffer. In order to control the conductivity of the medium buffer, 8.5% sucrose and 0.3% dextrose were mixed into the medium buffer in different ratios of either 20:1 or 45:1 such that the conductivity of the medium buffer could be adjusted to be either 72 or 5 $\mu\text{S}/\text{cm}$, respectively. In order to observe viable and non-viable cells under an optical microscope, the cell samples were labeled by trypan blue vital stain (Cambrex Corp., USA) indicator.

For the purpose of nucleus collection, a conventional boiling cell lysis process was performed at a temperature of 100°C for 5 min utilizing boiling water bath method. In order not to affect the medium solution, the thermal cell lysis process was performed out of the chip device. After the living cells were collected, they were moved out from the collection reservoir for cell lysis by using the pipette. Furthermore, to confirm the cell collection data, a commercial flow cytometry instrument (FACScan, BD Corp., USA) was employed to analyze the cell samples collected from both the chamber of viable and non-viable cell. For the confirmation of the separation efficiency of the proposed chip device, the cell samples were first labeled by DNA labeling fluorescent dye (PI, Propidium Iodide, Invitrogen Corp., USA) which is used to identify the viable/non-viable cells with the aid of a laser induced fluorescence (LIF) system after the separation process of the viable and non-viable cells utilizing DEP force, so that the properties of the cells will not be influenced by the fluorescent dye.

3 Results and discussion

3.1 Characterization of the microvalves/micropumps

The performance of the microvalves and micropumps were first investigated. Figure 4 shows the experimental results of the micro-pneumatic valve structure. As described earlier, two PDMS layers and a glass substrate were used

to form the control chamber and the liquid channel. While the compressed air was injected into the upper control chamber, a deformation of the PDMS membrane was generated to shut down the fluid channel. Hence, by turning on one of the four micro-pneumatic valves, the sample flow can be directed into any specific collection chamber. Therefore, pneumatic microvalves can be used as a reliable approach to manipulate the sample flow and switch the samples into a specific microchannel (Yang et al. 2006). Figure 4(a) shows a SEM image of the SU-8 master mold of the micro-pneumatic valve. The depth and the width of the master mold were 100 μm and 500 μm , respectively. The distance between two electrode fingers is

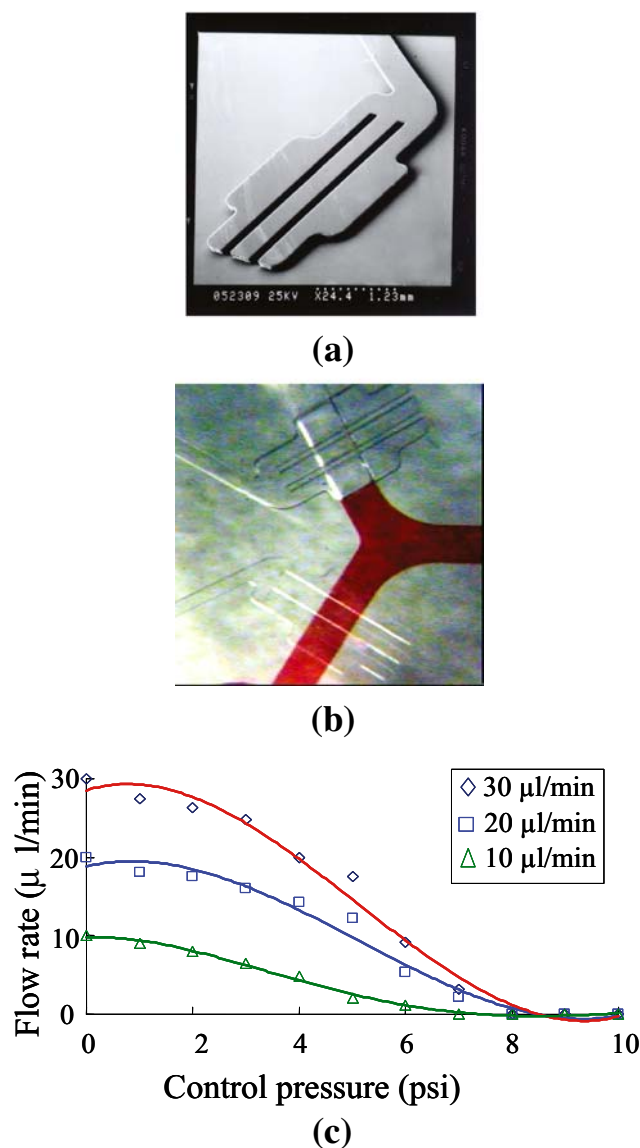


Fig. 4 (a) SEM image of the SU-8 master mold of the microvalve. (b) Microvalves are used to shut off fluid flows successfully. (c) The relation between initial flow rates and applied air pressure for the micro-pneumatic valve

100 μm . Note that the finger-type structure is designed to increase the area of the intersections between the valve structure and the liquid channel such that the micro-pneumatic valve can provide enough force to block the channel and control the sample flow. Figure 4(b) is a photograph showing that the micro-pneumatic valve can successfully block the fluid flow when compressed air was injected to activate the microvalve upwards. The relation between initial flow rates and applied air pressure for the micro-pneumatic valve is shown in Fig. 4(c). The applied control pressure to shut off the fluid is dependent on the initial flow rate. The higher the initial flow rate, the higher the air pressure required to completely shut off the sample flow. For example, for sample fluids with a flow rate of 30 $\mu\text{l}/\text{min}$, the air pressure required to actuate the micro-pneumatic valve is 10 psi.

In this study, we adopt a pneumatic micropump to transport cell samples. The S-shape pneumatic micropump is capable of generating reasonable pumping rates while using a single EMV and a simple control circuit. The performance of the micro-pneumatic pump has been investigated in our previously work (Yang et al. 2006).

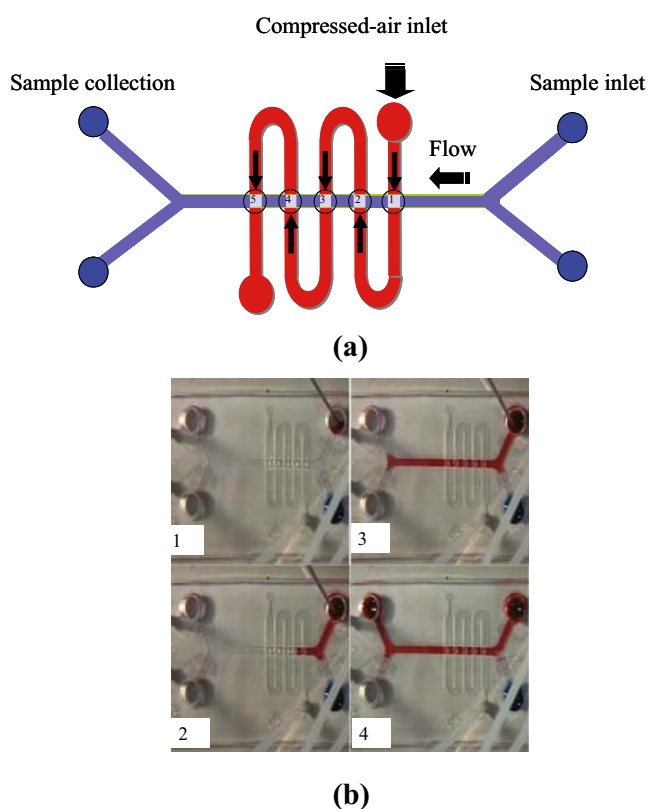


Fig. 5 (a) The schematic illustration of the S-shape micropump. Double-layer PDMS structures are used to construct the micropump, including an S-shape pneumatic microchannel, PDMS membrane structures, and a liquid microchannel. (b) Photographs of the operation process of the S-shape micropump

Figure 5(a) is a schematic illustration of the S-shape micro-pump. Similar to the microvalve structure, double-layer PDMS structures were used to construct the micropump device, including the S-shape pneumatic microchannel and a straight liquid channel located underneath. As shown in Fig. 5(a), the S-shape pneumatic microchannel intersects the liquid channel. The distance between each neighboring intersection area is designed to be 500 μm . The width and depth of the pneumatic microchannel are 500 and 100 μm , respectively. PDMS membrane structures were located at each intersection area and were deformed when compressed air flows through the S-shape pneumatic microchannel. The time-phased deformation of successive membranes creates a continuously peristaltic effect which drives the sample fluid to flow along the liquid channel. Instead of using three EMV switches, which is a common configuration for typical peristaltic micropumps, only one EMV switch was required in this design. The increase in the driving frequency and air pressure can enhance the pumping rate of the S-shape micropump. The pumping rate could reach a saturated value at a certain operation frequency. The pumping rate reaches a saturation value at a certain operation frequency (28 Hz). The experimental results show that the pumping rate of the micropump is 39.8 $\mu\text{l}/\text{min}$ at a pressure of 25 psi and a frequency of 28 Hz. At a zero flow rate, the micropump was measured to have a maximum back pressure of 0.019 psi (Wang and Lee 2005). Figure 5(b) shows a series of photographs indicating that the S-shape micro-pneumatic pump successfully transports sample flow continuously into the specific sample collection chamber. Note that dyes are used to improve visual observation.

3.2 Separation and collection of cells/nucleus

Cell and nucleus manipulation by using DEP forces were successfully demonstrated as shown in Fig. 6. In order to generate the DEP forces, several crucial operation parameters need to be considered, including the applied voltage, the operation frequency, and conductivity and permittivity of the medium buffer (Pohl 1978). In the following experiments, cell samples were first suspended in DMEM buffer, and the operational voltage and frequency applied to the DEP microelectrode structure were 15 $V_{\text{p-p}}$ and 16 MHz, respectively. During device operation, after the cell culture process, the mixed samples (including viable and non-viable cells) were first suspended in DMEM buffer with a conductivity of 72 $\mu\text{S}/\text{cm}$ and were transported to the microelectrode region by using the micro-pneumatic pump and microvalves (shown in Fig. 6(a)). The viable and non-viable cells were first randomly suspended around the microelectrode array region in the micro-sample flow channel. When the positive DEP forces were generated,

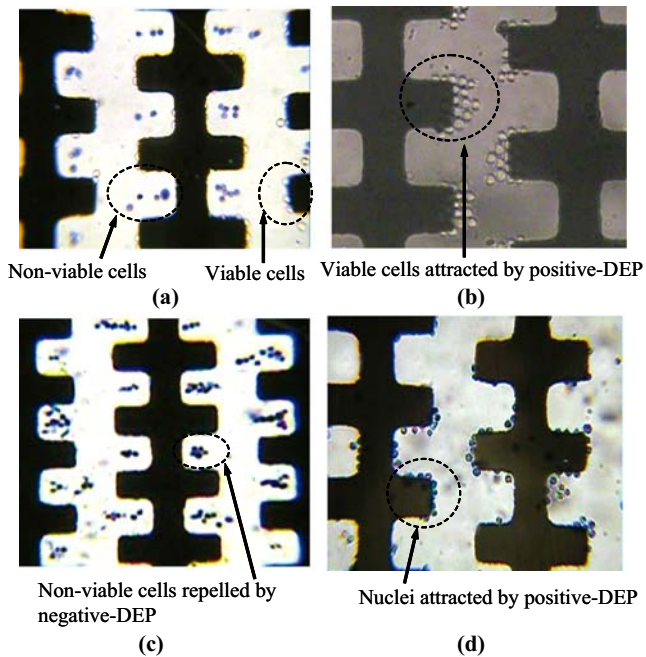


Fig. 6 The manipulation of human lung cancer cells and nucleus by using DEP forces. The purification of the viable and non-viable cells can be performed utilizing a microelectrode array (a). Viable cells are first placed around the DEP electrodes and then captured at the edge of microelectrodes by the positive DEP forces (b). Similarly, non-viable cells are first placed around the DEP electrodes and then repelled to the region between two electrodes where negative DEP forces are induced (c). Furthermore, the nucleus can be transported to the DEP electrodes and then attracted at the edge of the microelectrode structure by the positive DEP forces (d)

the viable cells were captured and collected at the edge of microelectrodes, as shown in Fig. 6(b). Alternatively, negative DEP forces were induced to repel the non-viable cells to the region between two electrodes (see Fig. 6(c)) and the non-viable cells were then transported to the subsequent collection chamber by using the micro-pneumatic pump/valves. After separation of the non-viable cells, the AC power supply was shut off and the viable cells were released from the microelectrode and then were collected to the viable cell collection chamber. Furthermore, after a thermal cell lysis process, nuclei, membranes, and cytoplasm can be separated using the same microfluidic chip. The micropump and microvalves can be used to transport these mixtures back to the DEP microelectrode array. Similarly, the DEP microelectrode structure was used to purify nuclei from the mixed sample flow. At a conductivity of $5 \mu\text{S}/\text{cm}$, an operational voltage of $15 V_{\text{p-p}}$, and an operational frequency of 200 kHz , the nuclei can be attracted at the edge of the microelectrode structure by the positive DEP forces effect (shown in Fig. 6(d)). The similar scheme can be used for nuclei collection utilizing the micro-pneumatic pump/valves devices.

A commercially available flow cytometer which is a popular technology used to identify and analysis biological molecule labeled with specific fluorescent dye (Edwards et al. 2004; Rieseberg et al. 2001) was then used to confirm the separation efficiency of the developed microfluidic platform. The analysis results are shown in Fig. 7(a) and (b). For the fluorescence detection, the cell samples were first labeled by PI after the separation process and draw out from the collection chamber. Because of the damage on the surface of the plasma membrane, the fluorescent dye can enter the non-viable cells, so that the signal amplitude of the non-viable cells can be larger than the viable cells under the fluorescence detection utilizing LIF system. As shown in Fig. 2, the magnitude of the positive DEP forces varies inside the microchannel (Rousselet et al. 1998). Briefly, the DEP force decreases as cells are away from the channel

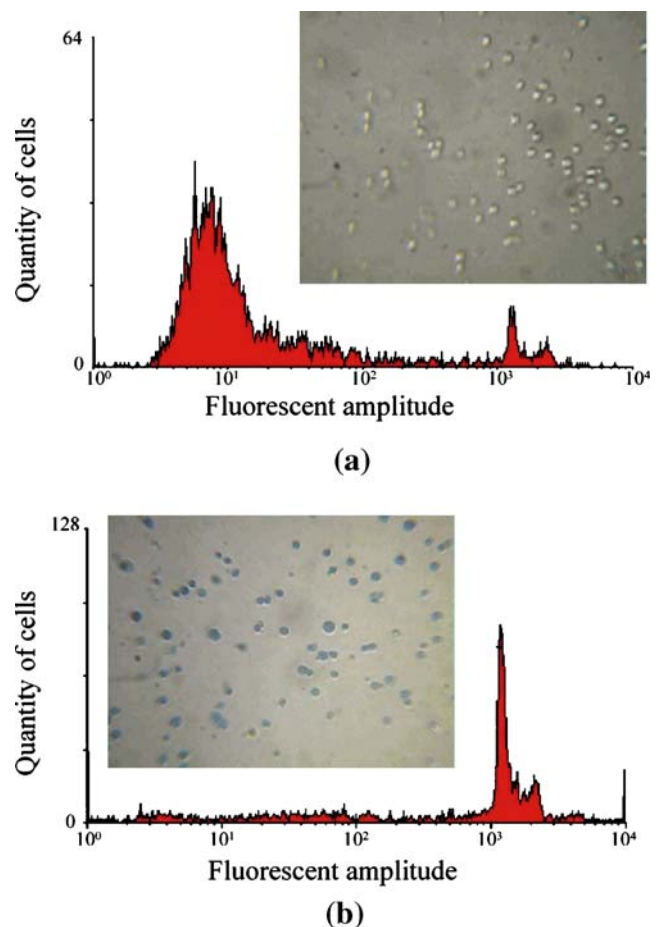


Fig. 7 The fluorescence signals detected by a conventional flow cytometry instrument of the viable (a) and non-viable lung cancer cells (b) labeled by the DNA labeling fluorescent dye (PI). Photographs in Fig. 6(a) and (b) represent the viable cells and non-viable cells inside the collection chambers. Note the non-viable cells are labeled by the trypan blue indicator, and can be observed under an optical microscope

Table 3 Experimental results of separation efficiency of the viable and non-viable cells confirmed by the commercial flow cytometry device

	Viable cells	Non-viable cells	Separation efficiency (%)
Viable cell collection chamber	3,379	641	84
Non-viable cell collection chamber	740	3,080	81

wall. In this study, the cell samples were suspended in the medium randomly. The cells near the bottom of the microchannel (h_1) can be attracted by the positive-DEP immediately. However, the cells far away from the microchannel (h_4) moving at a higher velocity may not be attracted towards the microelectrodes since the positive DEP force is too small. An average value of cell separation efficiency is 82.4% for ten experiments. The variation of the separation efficiency is 5.0%.

Likewise, the efficiency of the non-viable cells is 81% by using a single operation process, and the sampling quantity was 4,000 and 3,800 from viable and non-viable cell collection chambers, respectively. The photographs shown in Fig. 7(a) and (b) are of the viable cells (transparent) and non-viable cells (dark blue) inside the collection chamber, respectively. For the cell separation process, the initial flow rate was 3 $\mu\text{l}/\text{min}$ provided by the micropump device. The total volume of the starting sample was 100 μl containing about 8,000 cell samples, which was confirmed by a commercial flow cytometry counting process (as shown in Table 3). Therefore, number of cells per unit volume was calculated to be 80 cells/ μl approximately. The average efficiency of nuclei separation was 78.5%, which was confirmed by using commercial flow cytometry. Note the non-viable cells were labeled by the indicator of trypan blue, and could be observed under a microscope. Note that the separation efficiency can be enhanced if the separation and collection process are repeated several times.

4 Conclusion

In this study, we have successfully developed an automatic platform for cell/nucleus separation and collection utilizing DEP forces in a microfluidic system composed of a pneumatic micropump and four microvalves. By using MEMS fabrication technology, microfluidic devices were integrated onto the biochip to achieve the functions of cell sample transportation, separation and collection. A maximum pumping rate of 39.8 $\mu\text{l}/\text{min}$ can be achieved at a control pressure of 25 psi and at a driving frequency of 28 Hz. The microvalve can successfully shut off the sample flow. Finally, human lung cancer cells were used to demonstrate the functionality of the developed system. The separation efficiency of the viable and non-viable cells was confirmed to be 84 and 81%, respectively. Furthermore, nuclei can be also separated from membranes and

cytoplasm using the similar scheme. Experimental data showed that the developed microfluidic system can transport the cell samples, separate living cells from dead cells, and collect all living cells for further separation of cell nucleus from other organelles. Nucleus after cell lysis can be also separated and collected using the developed system with similar approach. The developed microfluidic system could provide a powerful tool for separation and collection of cells and nucleus, which is a useful platform for nuclear protein extraction and nuclear receptor binding assays.

Acknowledgements The authors gratefully acknowledge the financial support provided to this study by the National Science Council in Taiwan and by the MOE Program for Promoting Academic Excellence of Universities (EX-91-E-FA09-5-4). Also, the access provided to major fabrication equipment at the Center for Micro/Nano Technology Research, National Cheng Kung University is greatly appreciated.

References

- J.R. Anderson, D.T. Chiu, R.J. Jackman, O. Cherniavskaya, J.C. McDonald, H. Wu, S.H. Whitesides, G.M. Whitesides, *Anal. Chem.* **72**, 3158 (2000)
- J. Auerswald, H.F. Knapp, *Microelectron. Eng.* **67–68**, 879 (2003)
- P.A. Auroux, D.R. Reyes, D. Iossifidis, A. Manz, *Anal. Chem.* **74**, 2637 (2002)
- A.S. Bahaj, A.G. Bailey, in *Proceedings of the Industry Applications Society (IEEE) Annual Meeting*, Cleveland, OH, 1979, p. 154
- F.F. Becker, X.B. Wang, Y. Huang, R. Pethig, J. Vykoukal, P.R.C. Gascoyne, *Proc. Natl. Acad. Sci. U. S. A.* **92**, 860 (1995)
- M. Brown, C. Wittwer, *Clin. Chem.* **46**, 1221 (2000)
- N.H. Chiem, D.J. Harrison, *Clin. Chem.* **44**, 591 (1998)
- Y.J. Chuang, M.L. Tsai, S.H. Chen, *Electrophoresis* **27**, 4158 (2006)
- I. Doh, Y.H. Cho, *Sens. Actuators A* **121**, 59 (2005)
- D.C. Duffy, J.C. McDonald, O.J.A. Schueller, G.M. Whitesides, *Anal. Chem.* **70**, 4974 (1998)
- B.S. Edwards, T. Oprea, E.R. Prossnitz, L.A. Sklar, *Curr. Opin. Chem. Biol.* **8**, 392 (2004)
- L.M. Fu, G.B. Lee, Y.H. Lin, R.J. Yang, *IEEE/ASME Trans. Mechatron.* **9**, 377 (2004)
- P.R.C. Gascoyne, X.B. Wang, Y. Huang, F.F. Becker, *IEEE Trans. Ind. Appl.* **33**, 670 (1997)
- C.F. Gonzalez, V.T. Remcho, *J. Chromatogr. A* **1079**, 59 (2005)
- Y. Huang, R. Holzel, R. Pethig, X.B. Wang, *Phys. Med. Biol.* **37**, 1499 (1992)
- Y. Huang, K.L. Ewalt, M. Tirado, R. Haigis, A. Forster, D. Ackley, M.J. Heller, J.P. O'Connell, M. Krihak, *Anal. Chem.* **73**, 1549 (2001)
- K.K. Jain, *Trends Biotechnol.* **18**, 278 (2000)
- T.B. Jones, *Electromechanics of Particles* (Cambridge University Press, New York, 1995)
- T.B. Jones, *IEEE Proc. Nanobiotechnol.* **39**, 150 (2003)

- D.J. Laser, J.G. Santiago, J. Micromechanics Microengineering **14**, 35 (2004)
- G.B. Lee, C.H. Lin, S.C. Chang, J. Micromechanics Microengineering **15**, 447 (2005)
- H. Li, R. Bashir, Sens. Actuators B **86**, 215 (2002)
- C.H. Lin, G.B. Lee, B.W. Chang, G.L. Chang, J. Micromechanics Microengineering **12**, 590 (2002)
- A. Manz, D.J. Harrison, J.C. Verpoorte, H. Ludi, H.M. Widmer, in *Technical Digest IEEE Transducers '91*, San Francisco, 1990, p. 939
- G.H. Markx, M.S. Talary, R. Pethig, J. Biotechnol. **32**, 29 (1994)
- H.A. Pohl, J. Appl. Phys. **22**, 869 (1951)
- H.A. Pohl, J. Appl. Phys. **29**, 1182 (1958)
- H.A. Pohl, *Dielectrophoresis* (Cambridge University Press, Cambridge, UK, 1978)
- R. Raiteri, M. Grattarola, R. Berger, Materials Today **5**, 22 (2002)
- D.R. Reyes, D. Iossifidis, P.A. Aurox, A. Manz, Anal. Chem. **74**, 2623 (2002)
- K. Sato, A. Hibara, M. Tokeshi, H. Hisamoto, T. Kitamori, Adv. Drug Deliv. Rev. **55**, 379 (2003)
- M. Rieseberg, C. Kasper, K.F. Reardon, T. Scheper, Appl. Microbiol. Biotechnol. **56**, 350 (2001)
- A. Ring, M. Dowsett, Endocr.-Relat. Cancer **11**, 643 (2004)
- J. Rousselet, G.H. Markx, R. Pethig, Colloids Surf. A **140**, 209 (1998)
- T. Schnelle, T. Müller, G. Gradl, S.G. Shirley, G. Fuhr, Electrophoresis **21**, 66 (2000)
- P. Skehan, R. Storeng, D. Scudiero, A. Monks, J. McMahon, D. Vistica, J.T. Warren, H. Bokesch, S. Kenney, M.R. Boyd, J. Natl. Cancer Inst. **82**, 1107 (1990)
- P.L. Tazzari, A. Bontadini, F. Fruet, C. Tassi, F. Ricci, S. Manfroi, R. Conte, Vox Sang. **85**, 109 (2003)
- M.A. Unger, H.P. Chou, T. Thorsen, A. Scherer, S.R. Quake, Science **288**, 113 (2000)
- C.H. Wang, G.B. Lee, Biosens. Bioelectron. **21**, 419 (2005)
- C.H. Wang, G.B. Lee, J. Micromechanics Microengineering **16**, 341 (2006)
- X.B. Wang, Y. Huang, P.R.C. Gascoyne, F.F. Becker, R. Holzel, R. Pethig, Biochim. Biophys. Acta **1193**, 330 (1994)
- R.J. Widrow, C.D. Laird, Cytometry **39**, 126 (2000)
- R.J. Widrow, P.S. Rabinovitch, K. Cho, C.D. Laird, Cytometry **27**, 250 (1997)
- S.Y. Yang, S.K. Hsiung, Y.C. Hung, C.M. Chang, T.L. Liao, G.B. Lee, Meas. Sci. Technol. **17**, 2001 (2006)
- R. Zengerle, J. Ulrich, S. Kluge, M. Richter, A. Richter, Sens. Actuators A **50**, 81 (1995)
- B. Ziaie, A. Baldi, M. Lei, Y. Gu, R.A. Siegel, Adv. Drug Deliv. Rev. **56**, 145 (2004)
- H. Zou, S. Mellon, R.R. Syms, K.E. Tanner, Biomed. Microdevices **8**, 353 (2006)